THE SENSITIVITY OF AEROSOL SULFATE TO CHANGES IN NITROGEN OXIDES AND VOLATILE ORGANIC COMPOUNDS

Ariel F. Stein *
Department of Meteorology, The Pennsylvania State University
e-mail: ais5@psu.edu
Voice (301) 713-0295 x 119 Fax (301) 713-0119

1.0 INTRODUCTION

Traditionally, strategies to control sulfate formation have been focused on the response of sulfate (SO_4^{2-}) to reductions in sulfur dioxide (SO_2) emissions [e.g. Shin and Carmichael, 1992]. Much less attention has been devoted to assessing the effects on sulfate formation arising from changes in emissions of volatile organic compounds (VOC) and nitrogen oxides (NO_x), the chemical families largely responsible for the generation of the tropospheric ozone (O_3) and the oxidants needed to transform SO_2 to SO_4^{2-}. The response of ambient sulfate to reductions in NO_x and VOC emissions depends in part on the resulting changes in oxidant levels and the competition that naturally exists between in-cloud (*via* hydrogen peroxide) and clear-air (*via* hydroxyl radical) SO_2 oxidation. Coupling of the different chemical families leads to complex and potentially non-linear behavior with non-intuitive consequences (Stein and Lamb, 2000).

2.0 SO_4^{2-} SENSITIVITY TO NO_x AND VOC

The idea of "potential" sulfate can be utilized to study the combined response of aqueous- and gas-phase sulfate formation to changes in NOx and VOC emissions using one conceptual species only. Potential sulfate, defined as the sum of ambient sulfate (i.e. total sulfate) and hydrogen peroxide (H_2O_2) [Stockwell, 1994], can be interpreted as the maximum concentration of SO_4^{2-} that could be produced in the gas and aqueous phases. The usefulness of potential sulfate as a surrogate for ambient sulfate depends on the prevailing meteorological conditions and emission distributions. Nevertheless, this concept provides an integrated way to deal with this complex chemical system.

We can identify two photochemical regimes, each of which exhibits a different response of potential SO_4^{2-} production to changes in NO_x and VOC emissions, depending on the main sink of odd-hydrogen (HO_x), defined as the sum of hydroxyl (OH), hydroperoxyl (HO_2), and organic peroxyl (RO_2) radicals [Sillman, 1995]. When the formation of nitric acid (HNO_3) dominates the loss of odd-hydrogen, a decrease in NO_x frees up OH that can react with SO_2, CO, and VOC, which thus increases the abundance of HO_2 and in turn favors the formation of H_2O_2. Consequently, the interaction of these reactions tends to increase the formation of SO_4^{2-} via both the clear-air and aqueous-phase pathways. A decrease in VOC levels would reduce OH by making it available to form more HNO_3. As a consequence, the H_2O_2 production would also be reduced, thus decreasing the formation of SO_4^{2-}. Under this photochemical regime, called "VOC-sensitive", potential SO_4^{2-} decreases with decreasing VOC and *increases* with decreasing NO_x.

By contrast, when the formation of HNO_3 can be regarded as a small odd-hydrogen sink, a decrease in NO_x concentrations would slow down the conversion of HO_2 to OH, thereby decreasing the overall SO_4^{2-} formation. When the VOC levels are lowered, a small additional amount of OH would be available to react with SO_2, slightly increasing the gas-phase production of SO_4^{2-}. Lowering the VOC concentrations would not significantly affect the formation of H_2O_2, however, due to the fact that the system is saturated with hydrocarbons. Under this condition, changes in VOC levels would have little effect on HO_2 and hence on H_2O_2 formation [Sillman *et al.*, 1990]. Therefore, the aqueous-phase SO_2 oxidation would remain unaltered. This scenario constitutes the "NO_x-sensitive" photochemical regime, in which aerosol SO_4^{2-} concentrations would decrease with decreasing NO_x and would be largely independent of VOC. The highly nonlinear and coupled nature of the sulfate production process is responsible for this somewhat counter-intuitive behavior.

Milford *et al* [1994] and Sillman [1995] have developed a methodology to assess the sensitivity of a secondary pollutant (ozone) to changes in NO_x and VOC. They found that model predictions for O_3-NO_x sensitivity were associated with the concentrations of a number of key chemical species that differed from those linked to O_3-VOC sensitivity. Milford *et al*. [1994] showed that ozone simulated under an NO_x-sensitive regime was linked to afternoon values of total reactive nitrogen ($NO_y = NO_x + HNO_3$ + Peroxyacetylnitrates + alkyl nitrates) below a certain threshold concentration, while VOC-sensitive ozone was connected to higher NO_y levels. Sillman [1995] extended that work to include species ratios, such as O_3/NO_y and H_2O_2/HNO_3. Following these ideas, we propose the use of a combination of afternoon concentrations of HNO_3, H_2O_2,

* Corresponding author address: Ariel F. Stein, ARL – NOAA , 1315 East West Hwy, Silver Spring, MD 20910.

and ambient SO_4^{2-} as "indicator species" of the ambient SO_4^{2-}-VOC-NO_x sensitivity.

The link between the indicator value and the NO_x-VOC chemistry can be understood in terms of the dominant sinks and sources for odd-hydrogen. The NO_x-sensitive regime favors the formation of potential sulfate over the production of HNO_3. Under this condition the production of H_2O_2 constitutes the main loss of HO_x. Also, under NO_x-sensitive conditions the gas-phase SO_2 oxidation is favored over the formation of HNO_3. On the other hand, the VOC-sensitive regime is characterized by a high production rate of HNO_3 that overwhelms the formation of potential sulfate. Therefore, high values of the indicator ratio, $\{[H_2O_2]+[SO_4^{2-}]\}/\{[HNO_3]+[NO_3^-]\}$, are associated with NO_x-sensitive conditions while low values for the indicator can be identified with a VOC sensitive regime.

3.0 SIMULATION

In order to investigate the response of "potential" sulfate to changes in the NO_x and VOC source strengths we make use of U.S. Environmental Protection Agency (EPA)'s MODELS-3 [Dennis *et al*., 1996] Personal Computer (PC) version. This system constitutes a state-of-the-art tool for regional-scale simulations of photochemical smog, visibility and fine particulates. MODELS-3 is a versatile software system that includes a Community Multiscale Air Quality (CMAQ) model [EPA, 1999], a three-dimensional Eulerian chemical transport model that accounts for horizontal and vertical advection, eddy diffusion, gas-phase chemical transformations, emissions, cloud mixing, aqueous-phase chemical reactions, and aerosol processes. The meteorological data used by this simulation are obtained as output fields from the Mesoscale Model Version 5 (MM5) [Grell *et al*., 1994, Seaman and Michelson, 2000]. Emissions are calculated by the MODELS-3 Emissions Processing and Projection System (MEPPS) [EPA, 1999]. A detailed description of the equations and algorithms of each component of MODELS-3 are given by EPA [1999].

The simulation results presented here are based on an air pollution event that took place over the eastern United States during July 12-14, 1995. This episode featured concentrations exceeding the 1-h National Ambient Air Quality Standards (NAAQS) for ozone with a maximum of 175 parts per billion (ppb) measured at a Connecticut site on July 14 [Sistla *et al*., 2001]. In order to allow the model to build up the chemical species concentrations, thus minimizing the influence of initial conditions, the first two simulation days were treated as an initialization period. Therefore, only the results for July 14 are discussed here. The model domain covered an area of 2268 x 2808 km^2 from the Great Lakes and northern New England to the Gulf of Mexico with a 36-km resolution. The simulation utilized 15 non-hydrostatic sigma-pressure vertical layers. Initial concentrations and boundary conditions were set to near-rural conditions [Chang *et al*., 1990]. The RADM2 chemical mechanism [Stockwell *et al*., 1990] was used to simulate the gas-phase chemical reactions. The aerosol processes were calculated based on the Regional Particulate Model (RPM) [Binkowski and Shankar, 1995]. Area and point emissions were estimated using MEPPS, which is based on the 1995 National Emissions Trends [EPA, 1999]. Emissions data from motor vehicles and vegetation were simulated using the Mobile5a [EPA, 1996] and BEIS-2 [Pierce *et al*., 1998] models, respectively.

The meteorological data used for the present case study have been described in detail in Seaman and Michelson [2000], so only a brief summary is given here. This event featured light winds, restricted vertical mixing and high temperatures, conditions typically associated with a Bermuda high. Mesoscale structures associated with an Appalachian lee trough played a key role in determining the geographical distribution of photochemical smog. Low mixing depths and south-south-westerly flow favored the accumulation of photochemical precursors to the east of the trough [Seaman and Michelson, 2000], further explaining the observed ozone concentrations in excess of 120 ppb along the northeastern U.S. urban corridor.

The data used to verify the model predictions are a subset of measurements made during the North American Research Strategy for Tropospheric Ozone-Northeast (NARSTO-NE) 1995 intensive field campaign [Mueller, 1998]. A total of 327 measurement sites distributed throughout the Northeastern United States were selected to make the model comparison. The modeled and measured ozone concentrations were paired spatially by performing a bi-linear horizontal interpolation of the simulated values to the corresponding monitor locations.

4.0 RESULTS AND DISCUSSION

Good agreement is found between modeled and observed maximum 1-h ozone concentrations for the Northeastern U.S. The simulation captures the broad features of the geographical distribution of this episode, but not the detailed spatial variability. In particular, the highest ozone peaks are under-predicted by the model. The simulation shows a raw bias of –9.7 ppb, a normalized bias of –7.3%, a raw gross error of 18.3 ppb, and a normalized gross error of 18.5% for the spatially paired maximum 1-h ozone mixing ratios. These simulation results are within the performance "goals" suggested by Tesche *et al.* [1990] and by Hanna *et al.* [1996].

In order to build further confidence in the ability of the model to predict sensitivities of photochemical species to changes in VOC and NO_x, we performed three separate series of runs, each with 35% reductions in emission rates separately for VOC and NO_x. The first simulation (BASECASE) corresponds to the base case scenario with standard emission rates. In the second run (DBLSO2) the SO_2 emissions rates were doubled from those of the base case. In the third scenario (DBLVOC) the anthropogenic VOC emission rates were doubled with respect to the base case. Subsequently, we calculated the values for two concentration ratios, namely O_3/NO_z ($NO_z = NO_y$-NO_x) and H_2O_2/HNO_3, that are associated with ozone- NO_x- and VOC-sensitive locations at 16:00 EDT (20:00 UTC). VOC-sensitive locations are defined as those where the O_3 concentration in the simulation with reduced VOC is lower than the levels of O_3 in both the base case scenario and in the simulation with an equivalent reduction in NO_x by at least 5 ppb [Sillman *et al.*, 1997]. NO_x-sensitive locations are classified analogously. The median values along with the 5^{th} and 95^{th} percentiles for the indicator ratios corresponding to NO_x-sensitive and VOC-sensitive locations are not substantially different from those calculated by Sillman [1995; 1997]. NO_x-sensitive locations are associated with $O_3/NO_z > 12$ and $H_2O_2/HNO_3 > 0.5$, while VOC-sensitive stations are linked to $O_3/NO_z < 9$ and $H_2O_2/HNO_3 < 0.3$.

Following the methodology developed by Sillman [1995], we used the $\{[H_2O_2]+[SO_4^{2-}]\}/\{[HNO_3]+[NO_3^-]\}$ ratio as an indicator for the sensitivity of potential sulfate to changes in NO_x and VOC emissions. Figure 1 depicts the potential SO_4^{2-}-VOC-NO_x sensitivity for the BASECASE simulation at 16:00 EDT (20:00 UTC). This figure shows the percentage normalized reduction in $\{[H_2O_2]+[SO_4^{2-}]\}$ concentration as a consequence of either a NO_x or a VOC emission reduction for each grid within the model domain. The change in potential sulfate is plotted as a function of the concurrent indicator ratio, $\{[H_2O_2]+[SO_4^{2-}]\}/\{[HNO_3]+[NO_3^-]\}$. As can be inferred, there is well-defined contrast between NO_x and VOC sensitive locations. High $\{[H_2O_2]+[SO_4^{2-}]\}/\{[HNO_3]+[NO_3^-]\}$ ratios are associated with reductions in $\{[H_2O_2]+[SO_4^{2-}]\}$ concentrations as NO_x emissions are reduced, while no sensitivity is observed for changes in VOC (NO_x sensitive regime). On the other hand, low indicator ratios are linked to a decrease in "potential" sulfate as the VOC emissions are reduced and an *increase* in the $\{[H_2O_2]+[SO_4^{2-}]\}$ concentrations when the NO_x emissions decrease (VOC sensitive regime).

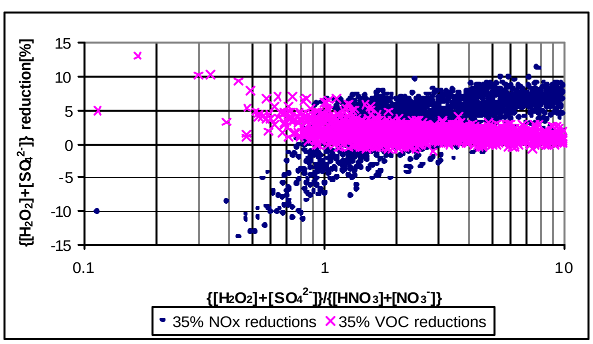

Fig 1 Normalized percentage response of potential sulfate concentrations to changes in NO_x and VOC versus $\{[H_2O_2]+[SO_4^{2-}]\}/\{[HNO_3]+[NO_3^-]\}$ ratios for 20:00 UTC, July 14, 1995.

The correspondence between the SO_4^{2-}-VOC-NO_x sensitivity and the indicator ratio was evaluated quantitatively by calculating the 95^{th} and 5^{th} percentiles for the $\{[H_2O_2]+[SO_4^{2-}]\}/\{[HNO_3]+[NO_3^-]\}$ ratios associated with VOC- and NO_x-sensitive locations respectively (Table 1). We define NO_x-sensitive locations as those where the normalized $\{[H_2O_2]+[SO_4^{2-}]\}$ calculated in the simulation with a 35% reduction in NO_x is lower than the normalized potential sulfate concentrations modeled with a 35% reduction in VOC by at least 5%. VOC-sensitive stations are defined in an analogous way. Table 1 also shows that the median values of the $\{[H_2O_2]+[SO_4^{2-}]\}/\{[HNO_3]+[NO_3^-]\}$ ratios linked to NO_x-sensitive stations are at least four times higher than those associated with VOC-sensitive locations. The 95^{th} percentile of the collection of indicator values corresponding to VOC-sensitive stations, which identifies the highest values for this distribution, along with the 5^{th} percentile of indicator values associated with NO_x-sensitive locations, reflecting the lowest values of the indicator distribution, identify the threshold interval of the $\{[H_2O_2]+[SO_4^{2-}]\}/\{[HNO_3]+[NO_3^-]\}$ ratio for the transition from VOC to NO_x sensitivity. The choice of these percentile cutoffs are based on Sillman *et al.* (1997). We find similar transition points for the three different model scenarios that range between 1.4 to 2.2.

Run	*VOC sensitive locations*		*NO_x sensitive locations*	
	50^{th} percentile	*95^{th} percentile*	*5^{th} percentile*	*50^{th} percentile*
BASECASE	0.96	1.82	1.54	7.30
DBLSO2	0.89	1.37	1.73	4.76
DBLVOC	1.23	2.25	1.60	7.46

Table 1 Distribution of $\{[H_2O_2]+[SO_4^{2-}]\}/\{[HNO_3]+ [NO_3^-]\}$ ratios for NO_x- and VOC- sensitive regimes.

5.0 CONCLUSIONS

MODELS-3 constitutes a suitable and powerful tool to assess the sensitivity of particulate sulfate to changes in primary pollutant source strength. In particular, the simulation results show that the response of potential sulfate levels to changes in VOC and NO_x emissions is strongly correlated with afternoon values of the $\{[H_2O_2]+[SO_4^{2-}]\}/\{[HNO_3]+[NO_3^-]\}$ indicator ratio. The relatively narrow range of the transition values unequivocally identifies either a VOC- or NO_x-sensitive regime despite the three different scenarios used in this modeling exercise. Under VOC-sensitive conditions (when the indicator ratio is less than approximately 1.4) potential sulfate is reduced when VOC emissions are reduced, but it is *increased* when NO_x emissions are reduced. On the other hand, under NO_x-sensitive conditions (values higher than 2.2 for the non-dimensional indicator) potential sulfate is reduced when NO_x emissions are reduced, while it is only weakly sensitive to changes in VOC.

6.0 REFERENCES

Binkowski F.S. and U. Shankar, The regional particulate model 1. Model decription and preliminary results, *J. Geophys. Res.*, 100, 26,191-26,209, 1995.

Chang J. S., F. S. Binkowski, N. L. Seaman, D. R. Stauffer, W. R. Stockwell, C. J. Walcek, S. Madronich, P. Middleton, J. E. Pleim, H. H. Landsford, The regional acid deposition model and engineering model. State of Science/ Technology Report 4, National Acid Precipitation Assessment Program, 722 Jackson Place, NW Washington D. C. 20503, 1990.

Dennis R.L., D.W. Byun, J.H. Novac, K.J. Galluppi, C.J. Coats, and M.A. Vouk, The next generation of integrated air quality modeling: EPA's MODELS-3, *Atmos. Environ.*, 30 (12), 1925-1938, 1996.

Environmental Protection Agency (EPA), Office of Mobile Sources: User's Guide for MOBILE 5a (Mobile Source Emission Factor Model), EPA-AA-TEB-92-01, 176 pp., 1996.

Environmental Protection Agency (EPA), Science Algorithms of the EPA MODELS-3 community Multiscale Air Quality (CMAQ) Modeling System, EPA/600/R-99/030. Office of Research and Development: Washington, DC 20460, 1999.

Grell G.A., J. Dudhia, and D.R. Stauffer, A description of the Fifth-Generation Penn State/NCAR Mesoscale Model (MM5). NCAR Tech. Note, NCAR/TN-398+STR, 122 pp., 1994.

Hanna S.R., G.E. Moore, and M.E. Fernau, Evaluation of photochemical grid models (UAM-IV, UAM-V, and the ROM/UAM-IV Couple) using data form the Lake Michigan Ozone Study (LMOS), *Atmos. Environ.,* 30 (19), 3265-3279, 1996.

Milford J.B., D. Gao, S. Sillman, P. Blossey, and A.G. Russell, Total reactive nitrogen (NOy) as an indicator of the sensitivity of ozone to reductions in hydrocarbon and NO_x emissions, *J. Geophys. Res.*, 99, 3533-3542, 1994.

Mueller P.K., NARSTO 1998 Model-Intercomparison study verification data: NARSTO-Northeast 1995 surface ozone, NO, and NO_x. Available online from the Langley Atmospheric Sciences Data Center, NASA Langley Research Center, Hampton, Virginia, U.S.A., 1998.

Pierce T., Ch. Geron, L. Bender, R. Dennis, G. Tonnesen, and A. Guenther, Influence of increased isoprene emissions on regional ozone modeling*, J. Geophys. Res*., 103 (D19): 25611-25629, 1998.

Seaman N.L. and S.A. Michelson, Mesoscale meteorological sturcture of a High-ozone episode during the 1995 NARSTO-Northeast study, *J. Appl. Meteorol.*, 39, 384-398, 2000.

Shin W-Ch., and G.R. Carmichael, Sensitivity of acid production/deposition to emission reductions, *Environ. Sci. Technol*., 26 (4), 715-725, 1992.

Sillman S., The use of NO_y, H_2O_2, and HNO_3 as indicators for ozone-NO_x-hydrocarbon sensitivity in urban locations, *J. Geophys. Res.,* 100 , 14175-14188, 1995.

Sillman S., J.A. Logan, and S.C. Wofsy, The sensitivity of ozone to nitrogen oxides and hydrocarbons in regional ozone episodes, *J. Geophys. Res.,* 95, 1837-1851, 1990.

Sillman S., D. He., C. Cardelino, and R.E. Imhoff, The use of photochemical indicators to evaluate ozone-NO_x-Hydrocarbon sensitivity: Case studies from Atlanta, New York, and Los Angeles, *J. Air Waste Manage. Assoc.*, 47, 1030-1040, 1997

Sistla G., W. Hao, J-Y. Ku, G. Kallos, K. Zhang, H. Mao, and S.T. Rao., An operational evaluation of two regional-scale ozone air quality modeling systems over the eastern United States, *Bull. Amer. Meteorol. Soc.,* 82, 945-964, 2001.

Stein A.F. and D. Lamb, The Sensitivity of Sulfur Wet Deposition to Atmospheric Oxidants. *Atmos. Environ.,* 34, 1681-1690, 2000.

Stockwell W.R., The effect of gas-phase chemistry on aqueous-phase sulfur dioxide oxidation rates, *J. Atmos. Chem.,* 19, 317-329, 1994.

Stockwell W.R., P. Middleton, and J.S. Chang, The second generation regional acid deposition model chemical mechanism for regional air quality modeling, *J. Geophys. Res.,* 95, 16343-16367, 1990.

Tesche T.W., P. Georgopoulos, J.H. Seinfeld, F. Lurmann, and P.M. Roth, Improvement in procedures for evaluating photochemical models. Report A832-103, California Air Resources Board, Sacramento, California, 1990.